nature climate change

SUPPLEMENTARY INFORMATION

https://doi.org/10.1038/s41558-017-0020-x

In the format provided by the authors and unedited.

The far reach of ice-shelf thinning in Antarctica

R. Reese[1,2], G. H. Gudmundsson[3], A. Levermann[1,2,4] and R. Winkelmann[1,2*]

[1]Potsdam Institute for Climate Impact Research (PIK), Member of the Leibniz Association, PO Box 60 12 03, Potsdam, Germany. [2]Institute of Physics and Astronomy, University of Potsdam, Potsdam, Germany. [3]British Antarctic Survey, Cambridge, UK. [4]Lamont–Doherty Earth Observatory, Columbia University, New York, NY, USA. *e-mail: ricarda.winkelmann@pik-potsdam.de

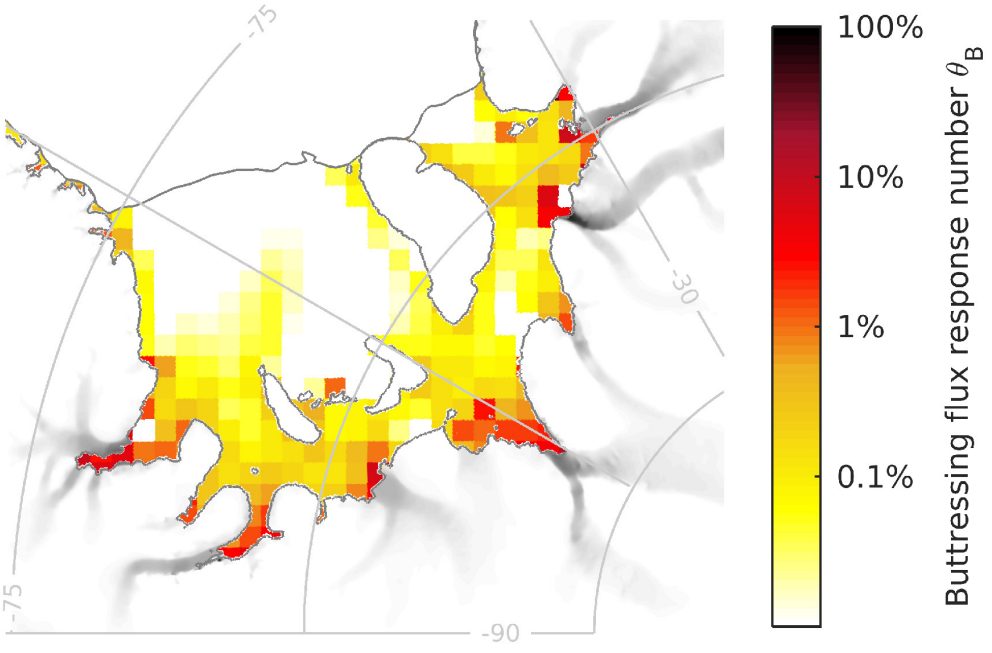

Fig. S1. Buttressing flux response numbers based on 40kmx40km perturbation areas for Filchner-Ronne Ice Shelf. As in Figure 1c, this figure shows the ratio of immediate change in ice flux across the grounding line over one year to the perturbation strength for Filchner-Ronne Ice Shelf. Here however, we perturb the ice shelf locally over 40kmx40km, i.e. areas four times as large as in Figure 1, showing that the buttressing response numbers do not depend significantly on the size of the perturbation areas.

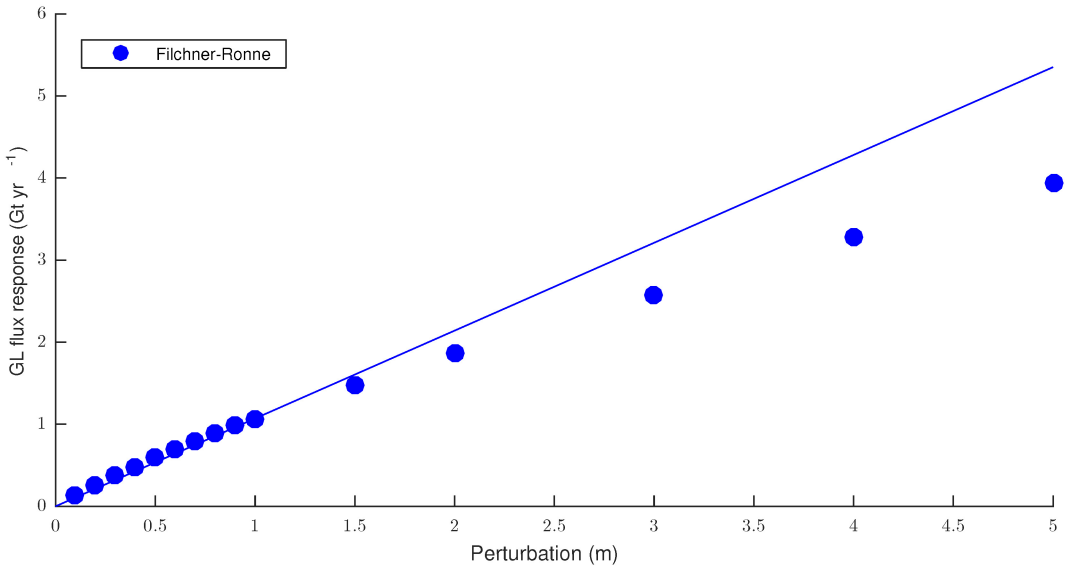

Fig. S2. Homogeneity range of the grounding line flux response. Shown is the modelled response for different uniform thickness perturbations of Filchner-Ronne Ice Shelf. The line indicates a linear function through the perturbation of 1m.

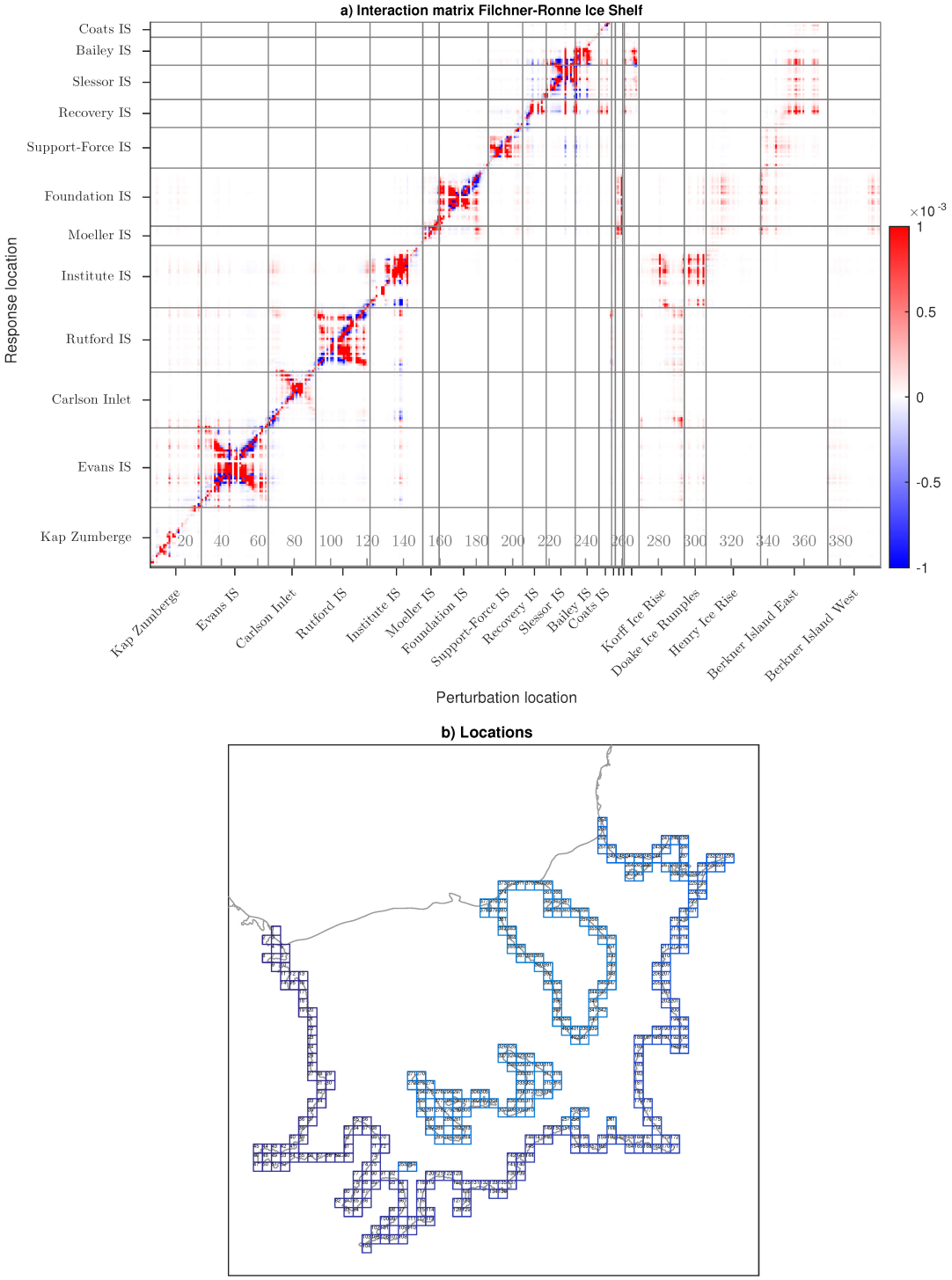

Fig. S3. Interaction matrix for Filchner-Ronne Ice Shelf. The interaction matrix (a) shows the flux response ratio in area *r* for a thickness perturbation in area *p*. Perturbation cells are numerated along the grounding line as shown in Panel (b). Neighboring squares are listed nearby. Colorbar shows the flux response ratio (red indicates flux increase, blue indicates reduced flux across the grounding line).

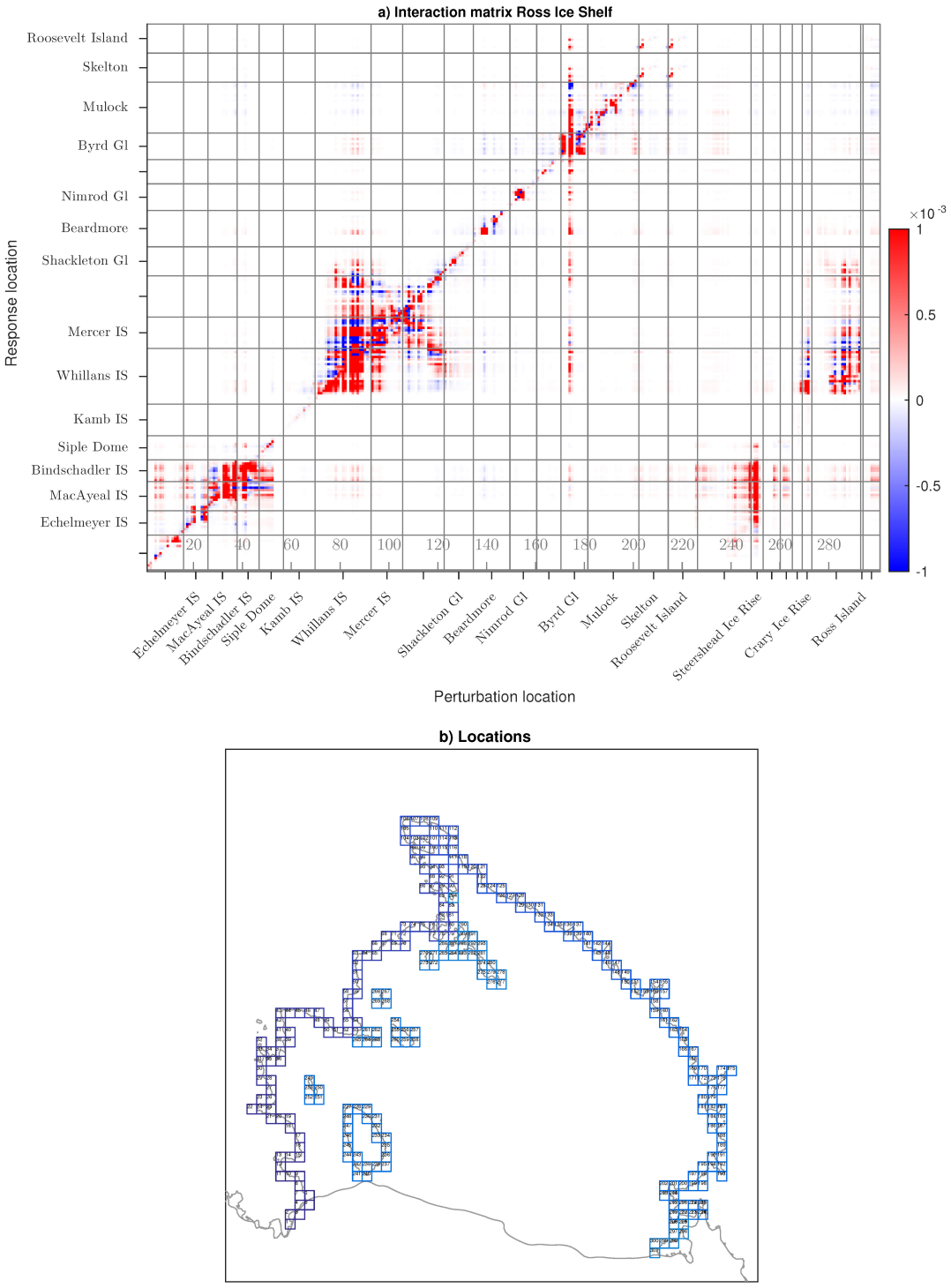

Fig. S4. Interaction matrix for Ross Ice Shelf. The interaction matrix (a) shows the flux response ratio in area *r* for a thickness perturbation in area *p*. Perturbation cells are numerated along the grounding line as shown in Panel (b). Neighboring squares are listed nearby. Colorbar shows the flux response ratio (red indicates flux increase, blue indicates reduced flux across the grounding line).

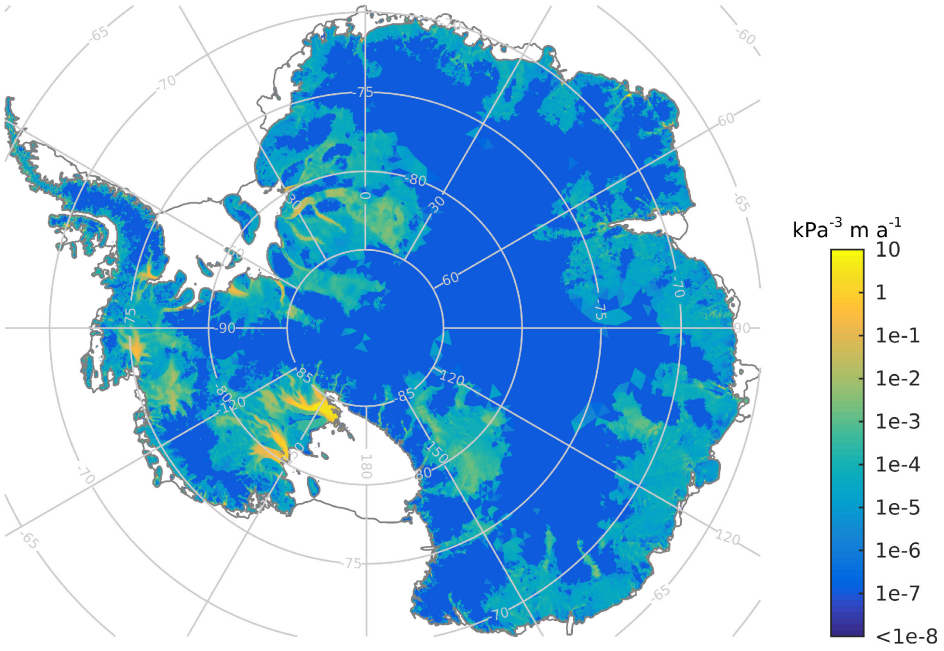

Fig. S5: Inverted slipperiness distribution. The basal slipperiness distribution is obtained by inversion with the ice-flow model Úa assuming a Weertman-type sliding law with exponent m=3. The slipperiness is an element based value; hence the patches visible in the interior are values of single elements.

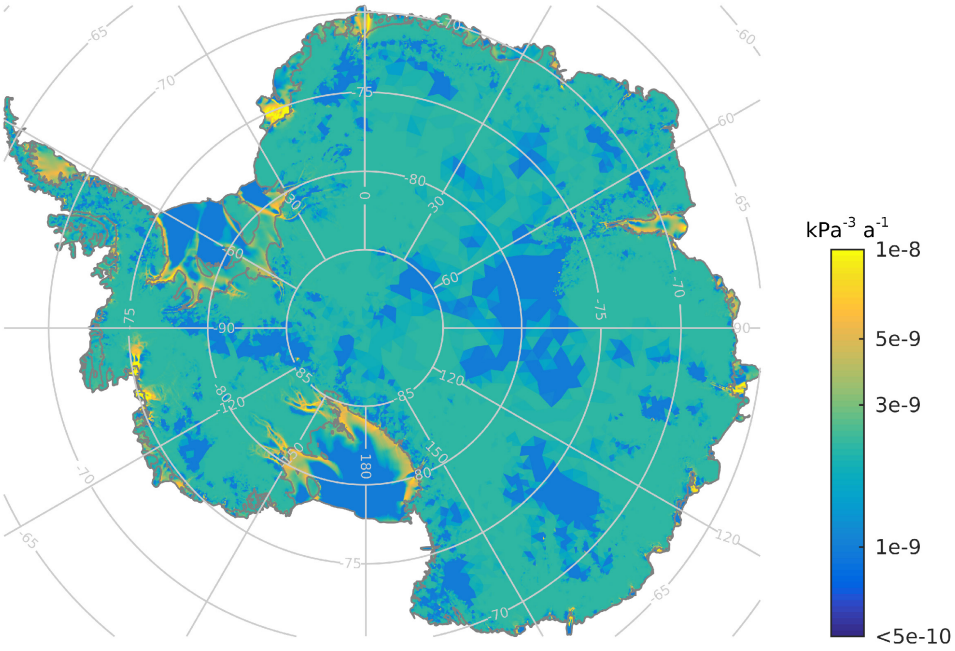

Fig. S6: Inverted ice rate factor. The ice rate factor A in Glen's flow law is estimated by inversion, assuming the exponent in Glen's flow law to be n=3. Similar as the basal slipperiness, the rate factor A is an element based quantity. The patches in the continent's interior are values of single elements.

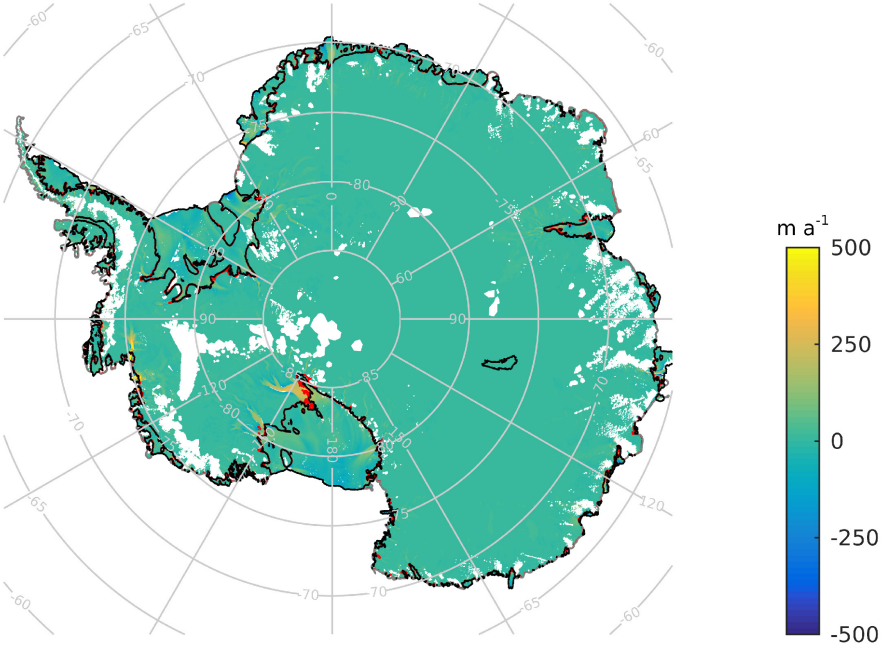

Fig. S7. Comparison of modelled and observed velocities and grounding line positions. The figure shows ice speed anomalies between the MEaSUREs data set[1] and model results from Úa. In the model, the speed is slightly underestimated in ice streams and overestimated towards the ice shelf fronts. Differences occur mostly in fast-moving stream regions. Masked areas are missing values in the data set. Grounding lines in the Bedmap2 data set[2] are shown in black and grounding lines in Úa in red (mostly superimposed with the back line). The average difference between modelled and observed ice speed is 43.8 meters per year with a median of 17.7 meters per year and a root mean square error of 93.8 meters per year.

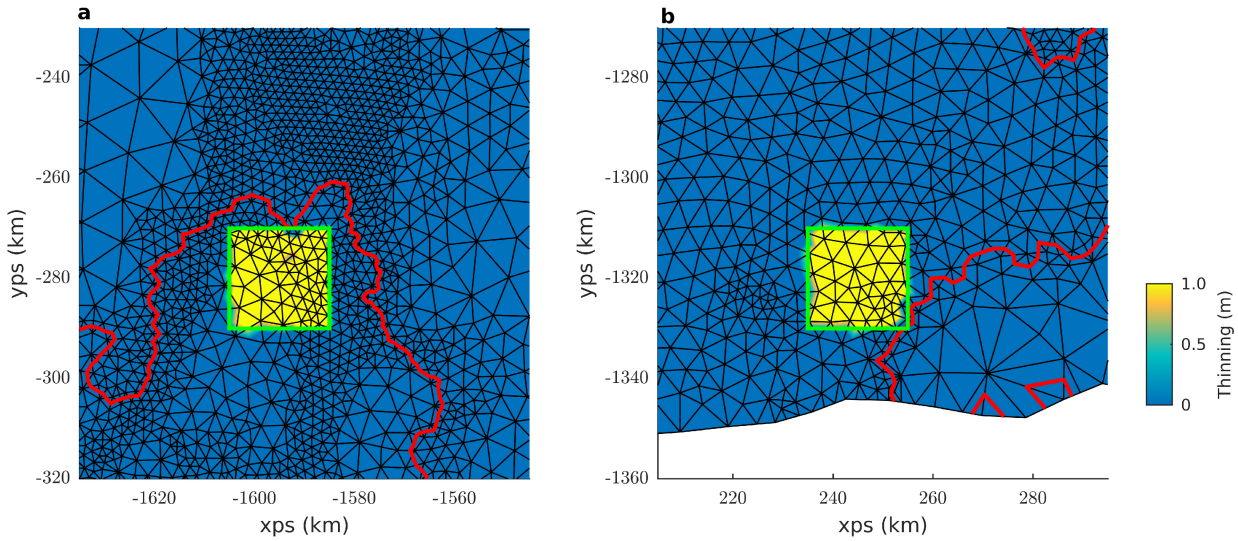

Fig. S8. Examples of perturbation areas. Shown is the perturbation (of 1m) in one exemplary perturbation cell (in yellow) for (a) the perturbed area in Figure 2a and (b) the perturbed area in Figure 2b. Red lines indicate the grounding lines, black lines the mesh. Nodes which belong to elements containing parts of the grounding line are not perturbed. This allows us to exclude possible effects of slope changes at the grounding line.

	Response (uniform) [Gt per yr]	Response (sum) [Gt per yr]	Area (perturbed) [km²]	GL flux [Gt per yr]
Filchner-Ronne	1.070	1.103	409,297	219
Ross	0.792	0.818	464,801	102
Crosson	0.454	0.471	1,899	35
George VI	0.312	0.312	20,115	85
Pine Island	0.285	0.287	4,712	102
Astrid & Ranghild	0.250	0.249	64,395	41
Shackleton	0.202	0.201	27,215	39
Amery	0.189	0.191	50,229	40
Getz	0.148	0.149	27,189	84
Dotson	0.143	0.127	3,002	10
Adélie	0.109	0.109	1,110	8
Larsen C, D	0.107	0.110	60,386	40
Venable	0.092	0.093	2,526	15
Abbot	0.080	0.089	26,634	23
West	0.075	0.077	14,129	44
Stange	0.057	0.059	6,288	16
Fimbul	0.047	0.050	36,562	21
Porpoise Bay	0.041	0.062	2,226	43
Riiser-Larsen	0.040	0.040	39,826	11
Thwaites	0.031	0.031	4,091	53
Mertz	0.027	0.027	4,858	14
Cook	0.025	0.023	2,949	26
Sulzberger	0.024	0.024	8,411	11
Brunt/Stancomb-Willis	0.019	0.019	34,286	24

Table S1. Additivity of the grounding line flux response. The uniform shelf response (column 1), obtained by uniformly perturbing the entire shelf by 1m, compares well with the summed shelf response (column 2), obtained by adding the responses of all perturbations of cells belonging to the ice shelf. The response is thus additive. The biggest ice shelves Filchner-Ronne and Ross show the overall highest response, but smaller ice shelves, e.g. near Pine Island Glacier or Crosson Ice Shelf in the Amundsen Sea, show a relatively high response compared to their area (column 3). For most ice shelves modelled fluxes (column 4) are slightly lower than observed fluxes[1].

References

1. Rignot, E., Mouginot, J. & Scheuchl, B. Ice flow of the Antarctic ice sheet. *Science* **333,** 1427–1430 (2011).

2. Fretwell, P. *et al.* Bedmap2: Improved ice bed, surface and thickness datasets for Antarctica. *The Cryosphere* **7,** 375–393 (2013).